The Impact of Two Types of El Niño on Northern Hemisphere upper Tropospheric Circulations in Summer Season

Karori, M. A.[1]

Abstract

The northern hemisphere (NH) stationary Circumglobal teleconnection (CGT) pattern in boreal summer season was identified and discussed in previous studies. The evidences were also found that the tropical thermal forcing can modulated this pattern. It is conceivable that warming in the eastern and central Pacific Ocean may influence the CGT pattern. The impacts of two types of El Niño on NH at 200 hPa height (H 200) have been investigated in this study. The observed data analysis revealed that the H200 anomalies are opposite in polarity during two types of El Niño Southern Oscillations (ENSO) i.e. Warm pool (WP) El Niño and Cold Tongue (CT) El Niño. During WP (El Niño), a zonal wave train is observed with phase opposite to that of well known CGT pattern in boreal summer season. During CT (El Niño) the Eurasian part is similar to the CGT pattern and opposite to that observed in WP El Niño. These contrasting impacts may be attributed to the different patterns of tropospheric warming and upper air divergence related to different convection centers in the Pacific Ocean during two types of El Niño. Moreover, negative anomaly of the central Asian High was observed during WP (El Niño), which may result in weaker summer monsoon over the south Asian region, especially over Pakistan and northwest India. A coupled general circulation model also simulated upper air wave patterns related to the two types of El Niño, which confirms our findings based on observed data analysis.

Introduction

The major teleconnection patterns over northern hemisphere (NH) in boreal winter season have been identified in many studies. For example, Horel (1981), Wallace and Gutzler (1981) found teleconnections by analyzing geopotential heights in the winter season; Branston and Livezey(1987) discussed the classification, seasonality and persistence of low frequency atmospheric circulation pattern; Pacific-East Asian teleconnection pattern in boreal winter season was discussed by Wang et al. (2000). These teleconnection patterns capture the tropical-extratropical interaction associated with peak phase of El Niño. Branstator (2002) also found a NH circumglobal waveguide pattern in boreal winter season by analyzing observed and model data. He showed that disturbances in the vicinity of strong jet are zonally oriented and those are meridionally oriented in the areas where the jet stream is weaker. During boreal summer season, the Asian jet stream is weaker which results in weaker teleconnection patterns. The sea surface temperature anomalies (SSTA) in the Pacific Ocean are also weaker since the mature stage of CT (El Niño) reaches in the boreal winter season (Rasmussen and Carpenter 1982). The phase locking of WP (El Niño) with annual cycle is less clear compared to the CT (El Niño) quantified by Niño-3 index (Weng et al. 2007). Hence the El Niño related teleconnection patterns are less clear in boreal summer than in boreal winter. However, some teleconnection patterns in NH in boreal summer have been reported in previous studies. For example, Branston and Livezey (1987) have identified three patterns; the North Atlantic Oscillations, Asian monsoon mode and a subtropical zonal mode. A Eurasian teleconnection pattern along Asian jet was pointed out (Joseph and Srinivasan 1999; Lu et al. 2002; Enomoto et al. 2003).Ding and Wang (2005) found by a boreal summer stationary Circumglobal teleconnection pattern on the basis of observed data analysis. They showed that the centers of action in CGT pattern are over the north-eastern Atlantic Ocean, west-central Asia, north-east Asia, central North Pacific Ocean and eastern Canada. Boreal summer CGT pattern has become a hot topic of interest. Many studies on summertime CGT have been carried out focusing on meteorological, climatological and prediction aspects (e.g. Blackburn et al. 2008, Li et al. 2008; Rajeevan and Sridhar 2008; Yadav 2009 a, b; Lin 2009; Yang et al. 2009; Yasui and Watanabe 2010). Ding et al. (2011) found that the leading mode of NH H200 which

[1]afzaalkarori@gmail.com
Pakistan Meteorological Department, Pitras Bukhari Road, Sector H-8/2, Islamabad, Pakistan

appears in summers preceding the peak phase of El Niño is CGT pattern and the one which appears in summers following peak phase of El Niño is western Pacific – North American (WPNA) pattern. They also pointed out that El Niño can modulate the both CGT and WPNA patterns indirectly. In a recent study, Wang et al. (2012) pointed out that the summertime CGT in NH has weakened since late 1970s. They attributed the weakening of CGT pattern in recent decades to the weakened coupling between Indian Summer Monsoon (ISM) rainfall and midlatitude circulations which further is a result of the reduced interannual variability of ISM rainfall due to changes in El Niño properties. In another study, Xie et al. (2012) discovered the signals of El Niño Modoki Index (EMI) (Ashok et al. 2007) on tropical tropopause and stratosphere. They pointed out a contrasting effect of two types of El Niño on middle-high latitude stratosphere. They also found that the contrasting effect is a result of complex interaction between Quasi-Biennial Oscillation (QBO) and El Niño Modoki signal.

In this study we investigated the impact of EMI on the CGT pattern and compared it with the impact of conventional El Niño. Thus, this investigation will help understand the mechanisms of tropical-extratropical NH teleconnection sin the context of different types of El Niño and the mechanism by which the effects of different locations of tropical Pacific warming centers reach remote regions. In this way the study will also help to improve the seasonal prediction of summer [Jun-July-August-September (JJAS)] monsoon season over Asian region.

Data and Methodology

The monthly mean datasets for the period 1950 – 2010 have been used, which include 1) the atmospheric dataset is from National Centers for Environmental Prediction–National Center for Atmospheric Research (NCEP/NCAR) reanalysis with resolution 2.5° × 2.5° (Kalnay et al., 1996). Geopotential height at 200 hPa from this data has been used, 2) Global Sea Surface Temperatures (SST) used in this study are from Hadley Center, HadISST with resolution 1° × 1° (Rayner et al. 2003). Many indices have been proposed to characterize WP El Niño and to differentiate it from the conventional El Niño. For example, WP (El Niño) Index (Kug et al. 2009), El Niño Modoki Index (Ashok et al.2007), Central-Pacific (CP) and Eastern-Pacific (EP) El Niño Indices (Kao and Yu 2009), CP and EP indices based on subsurface ocean temperatures (Yu et. al. 2010) etc. The latest one is proposed by (Renand Jin 2011). EMI given by (Ashok at el. 2007) has been used here to quantify WP (El Niño). EMI is defined as;

$$\mathrm{EMI} = \left[\mathrm{SSTA}\right]_{\mathrm{C}} - 0.5 \times \left[\mathrm{SSTA}\right]_{\mathrm{E}} - 0.5 \times \left[\mathrm{SSTA}\right]_{\mathrm{W}},$$

where square brackets with a subscript represent sea surface temperature anomaly (SSTA) averaged over a central region (C: 165°–140° W, 10°S–10° N), an eastern region (E: 110°–70° W, 15° S–5° N), and a western region (W:125°–145° E, 10° S–20° N). The CT El Niño has been quantified by Niño3.4 index, which is defined as the area average SST over the region (170°–120° W, 5° S–5° N).The choice of EMI is justified by Ashok et al (2007) and Weng et al (2007). The empirical orthogonal function (EOF) analysis of tropical Pacific Ocean SSTA for the period 1979 – 2008 provide a base to chose the above mentioned indices. The spatial patterns of two leading modes EOF1 and EOF2 resemble the conventional El Niño and EMI respectively (Figure not shown). The correlation between first principal component (PC1) and nino3 index (N3) is (0.96) and correlation between second principal component (PC2) and EMI is (0.98).The tropospheric temperature (TT) has been defined as the average atmospheric temperature between 700 – 200 hPa levels, following Goswami and Xavier (2005).

A significant change in CGT pattern in the latest decades has been reported by (Wang et al. 2012). A significant climate shift in the mid to late 1970s in tropical Indo-Pacific SSTs has also been reported (Terray 1994, Clark et al. 2000). Considering these facts we focused the study for the period 1979 to 2010.

Partial regression analysis has been used in this study to understand the influence of positive WP and CT (El Niño). Partial regression involves the calculation of linear dependence of a predict and on a predictor

by removing the effect of other coexisting phenomenon from both predictor and predict and, Moreover, the partial regression has been applied on the normalized time series of each predictor and predict and so that we may have comparable size of regression anomalies associated with the variations of predictor. Significance of the regression coefficient has been tested using two-tailed student's t-test. The number of degrees of freedom for seasonal partial regression was fixed at (N-3), N being the number of values in the time series. All the datasets used have been linearly detrended to focus the interannual variability.

CGT pattern

The CGT pattern is a global teleconnection pattern which exists at H200 in the NH in boreal summer season. This pattern has zonal wavenumber-5 structure. In this pattern, anomalous high (or ridge) centers are aligned zonally within 35°-45° N (Ding and Wang 2005). The structure is such that six centers of action exist, with positive anomaly over Western Europe, negative anomaly over European Russia, and positive anomaly over Central Asia, East Asian, North pacific and North America. The centers of action lie along the summertime jet stream in the NH.CGT index (CGTI) is defined as the areal average of NH H200 over the area (60°–70° E, 35°–40° N). The CGTI is independent of the area location within the region from 45° E to 80° E. Further details about CGT pattern can be found in (Branstator 2002; Ding and Wang 2005).The second leading EOF of NH H200 for the period 1951-2010 (Figure 1)represents the well know CGT pattern. This mode accounts for 13.4 % of total variance of NH H200. The spatial pattern of second EOF and explained variance is in accordance with (Ding and Wang, 2005; Wang et al. 2012). Figure 1b, shows the time expansion confident of second leading mode of NH H200 and CGTI. The linear correlation between H200 and CGTI for the period mentioned above is 0.57. The correlation is little bit reduced to 0.52 in recent decades i.e. 1979 – 2010. The correlation coefficient for both the periods is statistically significant above 99 % level on the basis of two-tailed student's t-test.

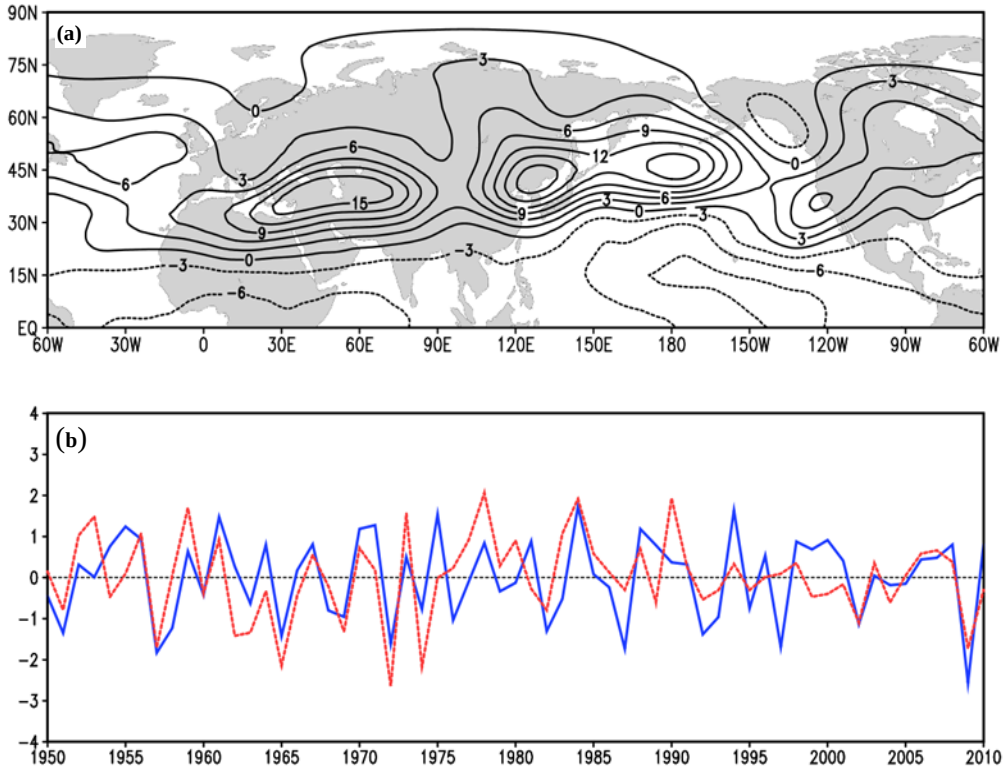

Figure 1: (a) The second EOF of JJAS H200 for the period 1950 – 2010. This pattern explains 13.4 % of the total variance. (Contour interval: 3 meter) **(b)** The normalized expansion coefficient of EOF-2 (Red solid line) and CGTI (H200 averaged over (60°–70° E, 35°–40° N)) (Red dashed line).

Result and Discussion

Impact of Two Types of El Niño

Figure 2 shows the pattern of CGT associated with two types of El Niño. There is a significant negative height anomaly over the North Atlantic and Western Europe during WP (El Niño) (Figure 2a). Eastern Europe and European Russian region lies under anomalous ridge while central Asian lies under negative height anomaly or in other words the central Asian anticyclone has become weaker in the events of WP El Niño. There is anomalous positive height further downstream over Northern Asia and East Asia. Across the Pacific from East Asia to North America a teleconnection pattern in observed, hereafter, we call it as East Asian – North American teleconnection (EANA). It may be noted that the CGT teleconnection pattern is positive-negative-positive from Northeast Atlantic to Central Asia, while in the case of WP (El Niño) the polarity is negative-positive-negative i.e. opposite to that of the Eurasian part of CGT (Figure 2a). It may also be noted that the NH H200 anomaly in the tropics is significantly negative all over the globe, except over the central Pacific Ocean during WP (El Niño).

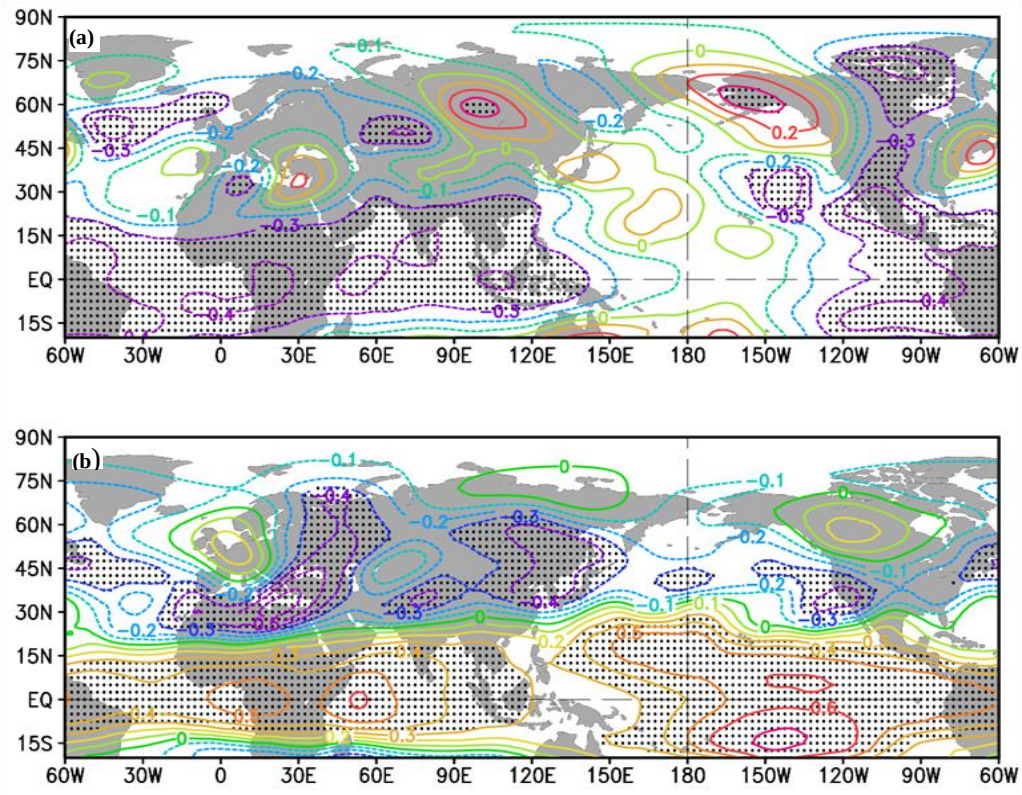

Figure 2: .Partial regression of H200 onto **(a)** EMI and **(b)** Niño 3.4 index. (Contour interval: 0.1, unit: standard deviation). The regions of statistically significant (90 % level) regression coefficients are stippled.

During CT (El Niño), the CGT pattern is opposite in polarity to that observed in case of WP (El Niño) (Figure 2b). The CGT pattern during CT (El Niño) is weaker in the study period as compared to that in the period 1950 – 1978. In that period the CGT is clearer with wavenumber-5 pattern (Figure not shown). This is in according with the previous study (Wang et al. 2012). However, the EANA part is still intact in the recent decades (Figure 2b). Moreover, the NH H200 anomaly in the tropics is positive all over the globe with maximum over the eastern Pacific, another maximum positive anomaly lies over the tropical western Indian Ocean. This emphasizes the contrasting response of NH H200 to the two types of El Niño. The Pacific North American (PNA) teleconnection pattern may

also be observed which is according to the previous studies (Horel and Wallace, 1981; Cai et al. 2011).

Discussion

Previous studies point out that change in the teleconnection pattern may be caused by changes in atmospheric latent heat patterns or changes in the mean background flow, especially the jetstream structure and boundary between mid latitude westerlies and tropical easterlies (Hoskins and Ambrizzi, 1993).The observed contrasting impacts of two types of El Niño on CGT may be because of changes in the tropospheric temperature patterns which emanate from different warming centers in the Pacific Ocean and associated latent heat released by convective precipitation. To investigate this we have partially regressed the TT and precipitation fields onto both the EMI and Niño 3.4 index (Figure 3).

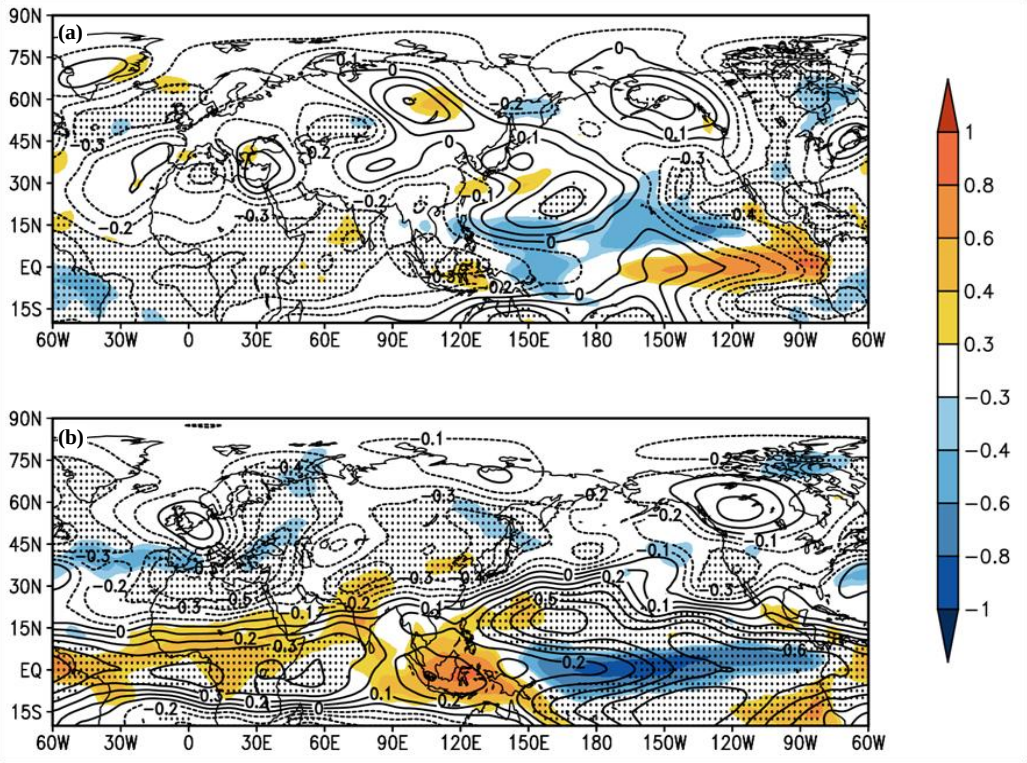

Figure 3: Partial regression of tropospheric temperatures TT (contours) and OLR (shaded) onto **(a)** EMI and **(b)** Niño 3.4 index (Contour interval: 0.1, unit: Standard Deviation). The regions of statistically significant (90 % level) regression coefficients of TT are stippled. Only statistically significant OLR anomalies are plotted.

The TT anomaly pattern associated with WP and CT (El Niño) is similar to the anomaly pattern observed for NH H200 (Figure 3a, b). This provides a clue that the two types of El Niño may impact the CGT by changing the TT anomaly pattern. Figure 3, also depicts the precipitation anomaly associated with two types of El Niño. The major difference of precipitation anomalies associated with two types of El Niño is that the maximum anomaly in the WP (El Niño) lies over the central Pacific and opposite anomaly is observed on the east and west side of the central maxima, while in CT (El Niño) there is a zonal dipole of precipitation anomaly over the equatorial Pacific Ocean. This anomaly pattern follows the SSTA pattern associated with two types of El Niño. Deep convection occurs over the anomalously warm SSTs. Latent heat released in deep convection warms the tropical troposphere and excites the pole ward propagating Rossby wave (e.g Wang et al., 2000; Weng et al., 2007; Weng et al., 2011; Feng and Li, 2011; Zhang et al. 2011; Cai et al. 2011 etc.), which is different in phase in two types of El Niño. The Rossby waves related to El Niño is called Pacific-East Asian teleconnection in the western Pacific and Pacific-North American teleconnection in the eastern

Pacific. The northeastward moving Rossby waves emanating from the equatorial Pacific, in boreal winter, are reflected from the North American jet and enter the North African-Asian (NAA) jet (Shaman and Tziperman, 2005). Once the disturbance enters the NAA jet, it is trapped in it and moves eastward affecting the weather and climate of regions in its way e.g. snow cover over Tibetan Plateau (Shaman and Tziperman, 2005). During WP El Niño boreal winters a subtropical jet (STJ) is activated and enhanced with origin in the west of that in CT (El Niño). The pole ward moving Rossby waves originating from central Pacific are trapped in this jet and move eastward affecting the regional weather of Europe (Graff and Zanchettin, 2012). No such eastward moving signal has been identified in boreal summer season (Shaman and Tziperman, 2007). The atmosphere in the upper troposphere responds to the tropospheric warming and upper air divergence over the equatorial pacific. Different location centers of upper air divergence and tropospheric warming (Figure 3) related to different centers of warm SSTs in the equatorial Pacific may give rise to contrasting response of CGT in two types of El Niño. During WP El Niño (Figure 2a and 3a) central equatorial Pacific warming may generate northwestward propagating signal in the upper air which results in reversed CGT pattern to that observed during CT El Niño (Figures 2b and 3b). Previous studies also have pointed out the interaction of NAA jet and westward propagating signal from the equatorial Pacific in boreal summer season (Shaman and Tziperman, 2007).

Summary

This study points out the contrasting impacts of two types of El Niño on NH CGT pattern in boreal summer season using the observed data. It has been hypothesized that tropospheric warming and upper air divergence, related to different warming centers in equatorial Pacific, is likely to cause the contrasting response of CGT pattern. There is a need to explain the underlying mechanism and to test the hypothesis on dynamical basis. Numerical simulation with WP and CT El Niño forcing may be carried out for future study. It is conceivable that phase shift of CGT in two different flavors of El Niño may have different impacts on regional climate along the action centers of CGT, especially South Asian summer monsoon which is highly correlated with CGT (Ding and Wang, 2005; Wang et al. 2012). Thus remote impacts of different types of El Niños via CGT on the climate of different regions may be explored.

References

Ashok, K., S. K. Behera, S. A. Rao, H. Y. Weng, T. Yamagata, 2007: El Niño Modoki and its teleconnection. J. Geophys. Res., 112, C11007, doi: 10.1029/2006JC003798.

Barnston, A. G., and R. E. Livezey, 1987: Classification, seasonality and persistence of low-frequency atmospheric circulation patterns. Mon. Wea. Rev., 115, 1083–1126.

Blackburn, M., J. Methven, and N. Roberts, 2008: Large-scale context for the UK floods in summer 2007. Weather, 63, 280–288.

Branstator, 2002: Circumglobal teleconnections, the jet stream waveguide, and the North Atlantic Oscillation. J. Climate, 15, 1893–1910.

CaiW., P. Rensch, T. Cowan, and H. H. Hendon, 2011: Teleconnection pathways of ENSO and the IOD and the mechanisms for impacts on Australian rainfall. J. Climate, 24, 3910 – 3923.

Clark, C. O., J. E. Cole and P. J. Webster, 2000: Indian Ocean SST and Indian summer rainfall: Predictive relationships and their decadal variability. J. Climate, 13, 2503 – 2519.

Ding, Q. H., and B. Wang, 2005: Circum global teleconnection in the Northern Hemisphere summer. J. Climate, 18, 3483–3505.

Ding, Q. H., and B. Wang, J. M. Wallace, and G. Branstator, 2011: Tropical–Extra tropical teleconnections in Boreal Summer: Observed Inter annual Variability. J. Climate, 24, 1878 – 1896.

Enomoto, T., B. J. Hoskins, and Y. Matsuda, 2003: The formation mechanism of the Bonin high in August.Quart. J. Roy. Meteor. Soc., 129, 157–178.

Feng, J., and J. Li, 2011: Influence of El Niño Modoki on spring rainfall over south China. J. Geophys. Res., 116, doi: 10.1029/2010JD015160.

Goswami, B. N., and P. K. Xavier, 2005: ENSO control on the south Asian monsoon through the length of therainy season. Geophys. Res. Lett., 32, L18717, doi:10.1029/2005GL023216.

Graff, H. F., and D. Zanchettin, 2012: Central Pacific El Niño, the "subtropical bridge,"and Eurasian climate. J. Geophys. Res., 117, D01102, doi: 10.1029/2011JD016493.

Horel, J. D., 1981: A rotated principal component analysis of the interannual variability of the Northern Hemisphere 500-mbheight field. Mon. Wea. Rev., 109, 2080–2092.

Horel, J. D., and J. M. Wallace, 1981: Planetary-scale atmospheric phenomena associated with the Southern Oscillation. Mon. Wea. Rev., 109, 813–829.

Hoskins, B. J., and T. Ambrizzi, 1993: Rossby wave propagation on a realistic longitudinally varying flow. J. Atmos. Sci., 50, 1661–1671.

Joseph, P. V., and J. Srinivasan, 1999: Rossby waves in Mayand the Indian summer monsoon rainfall. Tellus, 51A, 854–864.

Kalnay, E., and Coauthors, 1996: The NCEP/NCAR reanalysis project, Bull. Amer. Meteor. Soc., 77, 437-471.

Kao, H. Y., and J. Y. Yu, 2009: Contrasting eastern-Pacific and central-Pacific types of ENSO. J. Climate, 22, 615–632.

Karori, M. A., J. P. Li, and F.-F. Jin, 2013: Asymmetric influence of two types of El Niño and La Niña on summer rainfall over Southeast China. Journal of Climate.26, 4567 – 4582.

Kug, J. S., F. F. Jin, and S. I. An, 2009: Two types of El Niño events: Cold tongue El Niño and warm pool El Niño. J. Climate, 22, 1499–1515.

Larkin, N. K. and D. E. Harrison, 2005: On the definition of El Niño and associated seasonal average U.S. weather anomalies. Geophys. Res. Lett., 32, L13705, doi: 10.1029/2005GL022738.

Li, S., J. Perlwitz, X. Quan, and M. P. Hoerling, 2008: Modelling theinfluence of North Atlantic multi decadal warmth on the Indian summer rainfall. Geophys. Res. Lett., 35, L05804, doi: 10.1029/2007GL032901.

Lin, H., 2009: Global extra tropical response to diabetic heating variability of the Asian summer monsoon. J. Atmos. Sci., 66, 2697–2713.

Lu, R.-Y., J.H. Oh, and B.J. Kim, 2002: A teleconnection pattern in upper-level meridional wind over the North African and Eurasian continent in summer. Tellus, 54A, 44–55.

Rajeevan, M., and L. Sridhar, 2008: Inter-annual relationship between Atlantic sea surface temperature anomalies and Indian summer monsoon. Geophys. Res. Lett., 35, L21704, doi: 10.1029/2008GL036025.

Rasmusson, E. M., and T. H. Carpenter, 1982: Variations in tropicalsea surface temperature and surface wind fields associated with the Southern Oscillation/El Niño. Mon. Wea. Rev., 110,354–384.

Rayner, N. A., D. E. Parker, E. B. Horton, C. K. Folland, L. V. Alexander, D. P. Rowell, E. C. Kent, and A. Kaplan, 2003: Global analyses of sea surface temperature, sea ice, and night marine air temperature since the late nineteenth century. J. Geophys. Res., 108, No. D14, 4407, doi: 10.1029/ 2002JD002670.

Ren, H. L., and F. F. Jin, 2011: Niño indices for two types of ENSO. Geophys. Res. Lett., 38, L04704, doi: 10.1029/2010GL046031.

Shaman, J., and E. Tziperman, 2005: The Effect of ENSO on Tibetan Plateau Snow Depth: A Stationary Wave Teleconnection Mechanism and Implications for the South Asian Monsoons. J. Climate, 18, 2067 – 2079.

Shaman, J., and E. Tziperman, 2007: Summertime ENSO–North African–Asian Jet teleconnection and implications for the Indian monsoons. Geophys. Res. Lett., 34, L11702, doi: 10.1029/2006GL029143.

Terry, P., 1994: An evaluation of climatological data in the Indian Ocean area. J. Meteor. Soc. Japan, 72, 359 – 385.

Wallace, J. M., and D. S. Gutzler, 1981: Teleconnection in thegeopotential height field during the Northern Hemispherewinter. Mon. Wea. Rev.,109, 784–812.

Wang, B., R. G. Wu, and X. H. Fu, 2000: Pacific–East Asian teleconnection: how does ENSO affect East Asian Climate? J. Climate, 13, 1517-1536.

Wang, H., B. Wang, F. Huang, Q. Ding, and J. Y. Lee, 2012: Interdecadal change of the boreal summer circum global teleconnection (1958–2010). Geophys. Res. Lett., 39, L12704, doi: 10.1029/ 2012GL052371

Weng, H. Y., G. Wu, Y. Liu, S. K. Behera, and T. Yamagata, 2011: Anomalous summer climate in China influenced by the tropical Indo-Pacific Oceans. Climate Dyn., 36, 769-782.

Weng, H. Y., K. Ashok, S. K. Behera, S. A. Rao, and T. Yamagata, 2007: Impacts of recent El Niño Modoki on dry/wet conditions in the Pacific rim during boreal summer. Climate Dyn., 29, 123-129.

Xie, F., J. Li, W. Tian, J. Feng, and Y. Huo, 2012: Signals of El Niño Modoki in the tropical tropopause layer and stratosphere. Atoms. Chem. Phys., 12, 5259 – 5273. Doi: 10.5194/acp-12-5259-2012

Xie, P. P., and P. A. Arkin, 1997, Global precipitation: a 17-year monthly analysis based on gauge observations, satellite estimates, and numerical model outputs. Bull. Amer. Meteor. Soc., 78, 2539-2558.

Yadav, R. K., 2009a: Changes in the large-scale features associated with the Indian summer monsoon in the recent decades. Int. J. Climatol., 29, 117–133.

Yadav, R. K., 2009b: Role of equatorial central Pacific and northwest of North Atlantic 2-metre surface temperatures in modulating Indian summer monsoon variability. Climate Dyn. 32, 549–563.

Yang, J., Q. Liu, Z. Liu, L. Wu, and F. Huang, 2009: Basin mode of Indian Ocean sea surface temperature and Northern Hemisphere circumglobal teleconnection. Geophys. Res. Lett., 36, L19705, doi: 10.1029/2009GL039559.

Yasui, S., and M. Watanabe, 2010: Forcing processes of the summertime circum global teleconnection pattern in a dry AGCM.J. Climate, 23, 2093–2114.

Yu, J. Y., H. Y. Kao, T. Lee, and S. T. Kim, 2010: Subsurface ocean temperature indices for central-Pacific and Eastern-Pacific types of El Niño and La Niña events. Theor. Appl. Climatol.103, 337-344. doi: 10.1007/s00704-010-0307-6.

Zhang, W., F. F. Jin, H. Ren, J. Li, and J. X. Zhao, 2012: Differences in Teleconnection over the North Pacific and Rainfall Shift over the USA associated with two types of El Niño during Boreal Autumn. J. Meteor. Soc. Japan, 90(4), 535-552.

Zhang, W., F. F. Jin, J. Li, and H. Ren, 2011: Contrasting impacts of two-type El Niño over the western north Pacific during boreal autumn. J. Meteor. Soc. Japan, 89, 563-569.